# Ligand-Mediated Anticodon Conformational Changes Occur during tRNA Methylation by a TrmD Methyltransferase[†]

Joseph M. Watts,[‡] J. Gabruzsk,[§] and Walter M. Holmes*[,‡,||]

*Department of Biochemistry and Department of Microbiology and Immunology, Medical College of Virginia campus of Virginia Commonwealth University, Institute for Structural Biology and Drug Discovery, 800 East Leigh Street, Suite 212, Richmond, Virginia 23219, and Merck & Company Inc., Warsaw, Poland*

*Received September 2, 2004; Revised Manuscript Received February 14, 2005*

ABSTRACT: Orthologs of TrmD, G37 tRNA methyltransferases, have been analyzed with regard to post-tRNA binding events required to move the residue G37 in proximity to bound AdoMet for catalysis. This was approached initially by probing tRNA with T2 nuclease or Pb acetate in the presence, then absence, of *Escherichia coli* TrmD protein. Cleavage patterns clearly show that portions of the anticodon loop phosphodiester backbone are protected from cleavage only in the presence of sinefungin, a potent AdoMet analogue. This demonstrates that there must be considerable movement of the loop region and/or protein as the AdoMet site is occupied. Florescence energy transfer experiments were employed to better assess the movement of the G37 and G36 base residues in response to occupancy of the AdoMet site. When the *Streptococcus pneumoniae* TrmD protein was bound to synthetic $tRNA_1^{Leu}$ substituted with 2-aminopurine at positions 36 and 37, fluorescence energy transfer analysis showed that a decrease in 2-aminopurine fluorescence occurs only when AdoMet is present. Taken together, these results suggest that the base to be methylated by the TrmD protein is mobilized into the active center after tRNA binding only when the AdoMet site is occupied.

tRNA(m1G37)methyltransferases, which are the products of *trmD* genes in eubacteria, catalyze the transfer of the methyl group of AdoMet[1] to the N1 position of guanine 37, which is adjacent the anticodon loop (Figure 1). These proteins methylate only transfer RNAs which recognize codons starting with cytosine and, therefore, recognize only tRNA species with 5′guanine at positions 37 and 36 (36, *1*). Analysis of nonsubstrate tRNAs substituted with guanine at positions 36 and 37 become substrates for this enzyme in vitro (*2*). Recently, tRNA with A or G at position 36 was shown to be a substrate for *E. coli* TrmD, provided G37 was still present (*3*). Crystallographic and mutational analyses support the model of base-catalyzed extraction of the N1 proton, allowing the methyl group of *S*-adenosylmethionine (AdoMet) to be transferred to position 1 of the purine ring (*4*). This essential modification prevents translational frame-shifting and the production of aberrant protein products (*5*). The loss of this gene product has been shown in vivo to prevent the growth of *S. pneumoniae*, and increasing *trmD* gene expression resulted in a dose-dependent increase in growth rate (*6*). It has also been shown to be essential for maximal growth of *Salmonella enterica* (*7*), *E. coli* (*8*), and *Bacillus subtilis* (*9*).

In a previous communication, it was shown that the *E. coli* enzyme protects several sites in the phospodiester backbone of the tRNA anticodon stem loop against cleavage with nucleases, lead ,or iodine (*10*). In that study, protection of phosphodiester residues associated with G36 and G37 were not protected. Subsequently, a suitable analogue of AdoMet, sinefungin, recently became commercially available (Figure 1) and was employed in the study we report here. AdoMet could not be used in the earlier experiments since the reaction would proceed and footprinting could not be carried out. An important issue for these studies is the actual position of the unmodified residue G37 in the tRNA structure. If this base is in a quasi-stacked configuration in the AC loop, then some movement of G37 must occur to bring it near the deeply buried AdoMet residue in the TrmD protein cleft (*11*). Several published structures speak to this issue. The structure of a fully modified transfer RNA was first determined by Rich and Kim ($tRNA^{phe}$) and later by others (*11*−*15*). In this structure, position 37 is "Y base", which is turned outward from the AC helix loop. Modifications have been shown to change the structure of RNA by interfering with base-pairing (*16*, *17*), base-stacking (*18*), changing ribose sugar pucker (*19*), base intercalation (*20*), providing new hydrogen bonding (*21*), allowing for the canonical U33 "U-turn" (*22*), and introducing torsion in the sugar−phosphate backbone (*23*). The anticodon loop structure, in particular, has come under scrutiny as NMR solution

[†] This work was supported by grants to W.M.H. from the National Science Foundation and GlaxoSmithKline.

* Corresponding author: phone, (804) 828-2327; fax, (804) 827-3664; e-mail, holmes@hsc.vcu.edu.

[‡] Department of Biochemistry, Medical College of Virginia campus of Virginia Commonwealth University.

[§] Merck & Co., Inc.

[||] Department of Microbiology and Immunology, Medical College of Virginia campus of Virginia Commonwealth University.

[1] Abbreviations: AdoMet, *S*-adenosyl-L-methionine; AdoHcy, *S*-adenosyl-L-homocysteine; $m^1G$, methyl-1 guanosine; TrmD, tRNA-(m1G37)methyltransferase enzyme; $tRNA_1^{Leu}$, transfer RNA leucine-1; PAGE, polyacrylamide gel electrophoresis; IPTG, isopropyl thiogalactoside.

10.1021/bi0481038 CCC: $30.25 
Published on Web 04/08/2005

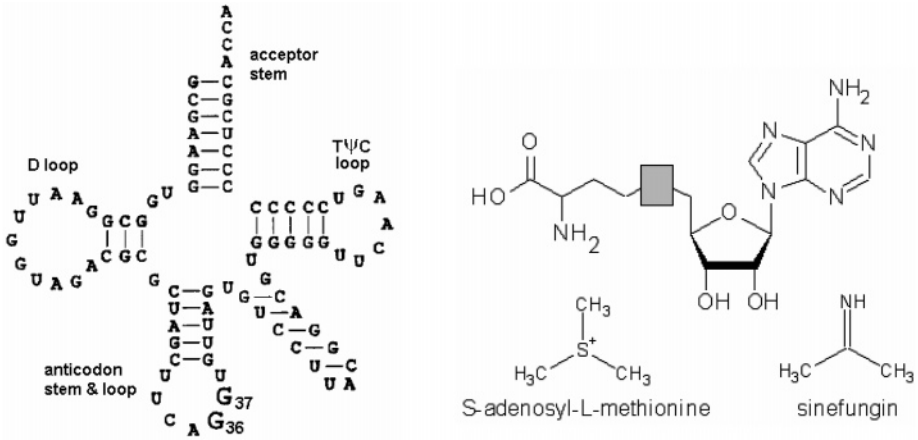


FIGURE 1: S-adenosyl-L-methionine (AdoMet) with its analogue sinefungin (right), and *Escherichia coli* $tRNA_1^{Leu}$ (left).

structures have presented a differing and more complex view of this region than previously seen. To date, the only available crystal structures are those of fully modified purified tRNA or tRNA bound to protein in a way that distorts the RNA's tertiary structure. Added complications to understanding actual structures in solution occur in crystals where RNA loops have base-paired across the crystal lattice. For example, base-pairing of the anticodon loop across the crystal lattice of a transcript has been observed in a structure of a $tRNA^{Phe}$ transcript bound by EF-Tu and GDPNp (*24*).

Recently, the solution structure of an unmodified, non-initiator $tRNA^{Met}$ anticodon stem (ASL) has been determined using NMR (*17*). This structure differs from that of the classic Kim $tRNA^{Phe}$ crystal structure. Here, the anticodon loop is in a stable A-form helix "triloop" with U33 base-pairing with A37. There is a complete lack of a U-turn, and the typically exposed bases 34−37 are protected from the solvent. Only upon dimethylallylation, does A37 turn out of the A-form helix and expose itself to solvent. In a subsequent publication, it was shown that this A37 modification stabilized the classic U-turn motif and exposure of anticodon loop bases in the presence of divalent cations or $Co(NH_3)_6^{3+}$. The unmodified ASL still did not adopt the classic U-turn in the presence of $Mg^{2+}$, $Mn^{2+}$, or cobalt-hexamine$^{3+}$ but displayed significantly more motion than in their absence (*25*). This observation is particularly interesting in the case of TrmD, as it has been shown that TrmD has an absolute dependency on the presence of $Mg^{2+}$ for catalysis (*2*, *6*). Perhaps the presence of divalent cations allows the tRNA anticodon freedom of movement such that bases 36 and 37 could be brought into the catalytic site by TrmD in the presence of *S*-adenosyl-L-methionine. The Agris group has shown, using NMR, that the G37 ASL modification leads to restriction of this base's ability to sample multiple environments, fixing G37 out into the solvent (*22*).

Here, we present evidence suggesting that the guanine bases of position G36 and G37 are mobilized near the active site of the enzyme only when AdoMet occupies its cognate binding site. In addition, we find major changes in the positioning of the phosphodiester backbone of the AC stem/loop. This idea is not without precedent, and recently, there have been reports of cocrystal structures of tRNA complexed with modifying enzymes, wherein specific RNA residues are moved in the complex. A cocrystal complex of TruB pseudouridine synthetase complexed with a T-loop RNA showed U55 (the modification site), C56, and G57R moved out of its helix and brought into a deep cleft rich in charged and aromatic residues (*26*). Archaeosine tRNA transglycosylase (ArcTGT), which modifies G15 in the D-arm, has been recently crystallized with a complete $tRNA^{Val}$ transcript, which shows that the D-arm of tRNAs is so completely turned out of its canonical form that it has been given a new nomenclature, the "lambda form" (*27*). In light of these recent findings, it should not be surprising that we observed tRNA structural changes in the TrmD proteins using enzymatic and chemical probes. Probes such as nuclease and lead target the phosphate backbone and give relatively little information about the potential environment of the bases themselves. It should be pointed out that neither of these two co-structures included other ligands. Therefore, the changes in tRNA structure seen in the ArcTGT tRNA complex could not require the presence of another ligand. It remains to be determined what structural changes might accompany the presence of queosine. In the case of the TruB enzyme, no addition ligands are necessary for the reaction to occur, but in this case, a fluorinated U55 residue presumably permitted stable complex formation required for crystallization.

One crucial tool used in studying the site-specific environmental changes of nucleotides is the use of fluorescent properties of 2-aminopurine. 2-Aminopurine is an analogue of adenine which fluoresces at neutral pH, a large range of ionic environments, and at ambient temperatures; changes in local environment can be used to reveal conformational transitions in polynucleotides (*28*). 2-Aminopurine has been extensively utilized in studying nucleotide environmental change in the case of AdoMet-dependent DNA methyltransferases using fluorescence energy quenching experiments (*29*−*31*). 2-Aminopurine causes minimal disruption to helical structures (*29*), has the ability to stack with neighboring bases (*32*, *33*), and has been shown to Watson−Crick base-pair with thymidine (*34*). Since 2-aminopurine has an excitation maximum above nucleotide absorption and below protein excitation and fluoresces at wavelengths above that of polypeptides, it is a good candidate for use in fluorescence resonance energy transfer (FRET) experiments (*35*). Here, we have utilized FRET analyses to examine changes in the environment of 2-aminopurine residues in tRNA when AdoMet is bound to tRNA−TrmD enzyme complexes.

## MATERIALS AND METHODS

*Cloning TrmD Orthologs.* The *trmD* gene from *E. coli* was cloned into a pET28 vector; N-terminally His-tagged protein was overproduced in BL21 (DE3) as previously described (*36*). The *Thermotoga maritima* gene was isolated and cloned as follows: genomic *T. maritima* DNA was used as template for PCR from genomic DNA provided by Dr. R. Huber, University of Wurtzburg, Germany. On the basis of a BLASTN (*37*) search of the *T. maritima* completed DNA sequence, specific primers for the *trmD* gene where synthesized and used for the amplification from *T. maritima* DNA template. The reaction mixture of 100 $\mu$L consisted of *T. maritima* DNA (0.5 $\mu$g), 1.6 $\mu$L (32 pmol) of each primer, upstream primer 5′-GC**GGATCC**AGAATCACAATAGTGAC-3′ containing a *Bam*H1 restriction site (bold) and downstream primer 5′-GCG**AAGCTT**CTAACATTTTTCCATCAAC-3′ containing a *Hind*III restriction site (bold) and stop codon (underlined), and 2 units of thermostable rTth polymerase. Buffer and dinucleotides were used as recommended by the manufacturer (Perkin-Elmer). Rounds of 30 cycles were performed with a temperature profile of 1 min at 95 °C, 1 min at 56 °C, and 1 min at 72 °C and then an additional 10 min extension at 72 °C was performed in a RoboCycler (Stratagene). The amplification products were analyzed by electrophoresis on a 1% agarose gel. The single DNA band of about 750 bp was excised from the agarose gel and purified by spin columns (Supelco). The PCR product was then cloned into pQE30 expression vector (Qiagen) to form pQE-THEMA. The pQE-THEMA construct was transformed into *E. coli* strain TG1 to produce the plasmid. The DNA sequence integrity was confirmed by DNA sequencing. To increase yields from this T5 promotor plasmid, we moved the His-tag and *trmD* gene into a T7 promotor vector. We subjected the pQE30-THEMA vector to enzymatic digestion at the *Eco*RI and *Hind*III sites, thereby preserving the gene product and His-tag sequence. The fragment was extracted from an agarose gel using the QIAEX-II gel extraction kit (Qiagen), and cloned into a pSP72 vector (Novagen), digested, and extracted with the same endonucleases (*Eco*RI and *Hind*III). The two products were ligated with T4 DNA ligase according to the manufacturer's directions (Stratagene), transformed into BL21(DE3) (Stratagene), selected for ampicillin resistance, plasmid-isolated, and sequenced using a primer specific to the T7 promotor. The resulting strains produced approximately 4 times as much enzyme per liter than the pQE-THEMA-containing strains upon induction with IPTG. The *S. pneumoniae* and *Staphylococcus aureus trmD* genes were cloned into a pET-15b vector (Novagen) as previously described (*6*) and were a generous gift of Magdalena Zalacain of GlaxoSmithKline.

*Enzyme Purification.* Enzyme was produced then purified over a nickel column as previously described (*4*) with the exceptions of induction at 18 °C rather than 25 °C and an addition of a wash step of 50 mM $PO_4$ buffer, pH 7.0, 300 mM NaCl, and 50 mM imidazole after binding to a Ni−NTA column (Qiagen). This purified product was extensively dialyzed twice in 50 mM Tris-HCl, pH 8.0, 100 mM KCl, 5 mM $MgCl_2$, 1 mM DTT, and 20% glycerin to remove enzyme-bound AdoMet, according to unpublished Biacore data from this lab. The proteins were filter-sterilized and stored at 4 °C in this buffer, with the exception of *T. maritima* TrmD which was more stabile at room temperature. Enzymes were used within two weeks of purification.

*tRNA Synthesis.* Transcript $tRNA_1^{Leu}$ was produced in vitro using T7 RNA polymerase as previously described (*2*). $tRNA_1^{Pro}$ with positions 36 and 37 substituted with 2-aminopurine was phosphoramidite-synthesized by CureVac, Germany. Both transcript and synthetic tRNA were resuspended in TE. To each, 1.1 mM $MgCl_2$ was added, then each was heated to 60 °C for 5 min and cooled to fold the tRNA.

*tRNA Labeling and Purification.* The $tRNA_1^{Leu}$ transcripts were 5′ -abeled with [$\gamma^{32}$P]ATP 5′ via a method outlined elsewhere (*38*) with the exception of replacing calf intestinal phosphatase with bacterial alkaline phosphatase (Sigma). 3′-Termini were labeled using terminal nucleotidyl-transferase and [$\alpha$-$^{32}$P]ATP according to protocols of Silberklang et al. (*39*). After phenol/chloroform extraction and ethanol/Na acetate precipitation, the labeled products were run on a 10% polyacrylamide 8 M urea gel. The labeled transcript was localized in the gel via autoradiography, and the band corresponding to labeled $tRNA_1^{Leu}$ was excised and either soaked overnight in a solution of 0.5 M ammonium acetate, 10 mM magnesium acetate, 0.1 M EDTA, and 0.1% (w/v) SDS or electoeluted. Following ethanol precipitation, we washed the labeled RNA with ice-cold 70% ethanol, dried, and resuspended in deionized water. Radiospecific activity was determined using a Packard Tri-Carb 1500 liquid scintillation counter.

*Gel Shift Assay.* Approximately 5 fmol of 5′ $\gamma$-phosphate-labeled $tRNA_1^{Leu}$ transcript (~20 000 cpm, as determined above) was added to increasing amounts of cloned TrmD protein from *E. coli*, *S. pneumoniae*, *S. aureus*, and *T. maritima* in 50 mM Tris-HCl, pH 8.0, 100 mM KCl, 5 mM $MgCl_2$, 5 mM 2-mercaptoethanol, and 10% glycerol. These mixtures were incubated for 15 min at 37 °C to determine a concentration of enzyme that would bind >97% of the tRNA on a 5% polyacrylamide native gel as described by David R. Setzer (*40*).

*Sinefungin Inhibition and Binding.* An 8 min assay containing 2 $\mu$M *S. pneumoniae* TrmD, 3.6 $\mu$M $tRNA_1^{Leu}$ transcript, and 15 $\mu$M *S*-adenosyl-L-methionine was carried out with varying concentrations of sinefungin. Half-maximal inhibition was seen in the presence of 50 $\mu$M sinefungin. A gel-shift assay was carried out as described above with the addition of 50 and 100 $\mu$M sinefungin concentrations to determine if addition of sinefungin caused any increase or decrease in enzyme binding.

*Footprinting with $Pb^{2+}$ and RNase $T_2$.* TrmD was dialyzed immediately before experiments against 0.01 M Tris-HCl buffer, pH 7.4. RNase $T_2$ was obtained from BRL. Experiments were conducted in 5 $\mu$L reaction mixtures with a $tRNA_1^{Leu}$ concentration of 1 $\mu$M and 50−200 $\mu$M. Transcript and enzyme were preincubated for 5 min, then the selected nuclease was added for 10 min. Digestions with nuclease RNase $T_2$ were carried out in 20 mM Tris-HCl buffer, pH 7.5, 10 mM $MgCl_2$, and 100 mM KCl. Reactions were terminated by phenol/chloroform extraction followed by ethanol precipitation. $tRNA_1^{Leu}$ transcript labeled at the 5′-terminus (30 000 cpm Cerenkov) was mixed with 4 $\mu$g of carrier tRNA then cleaved with freshly dissolved lead acetate. The reaction mixture contained increasing concentrations of TrmD (0−200 $\mu$M) in 20 mM Hepes−NaOH buffer, pH 7.5, 5 mM magnesium acetate, and 50 mM potassium acetate.

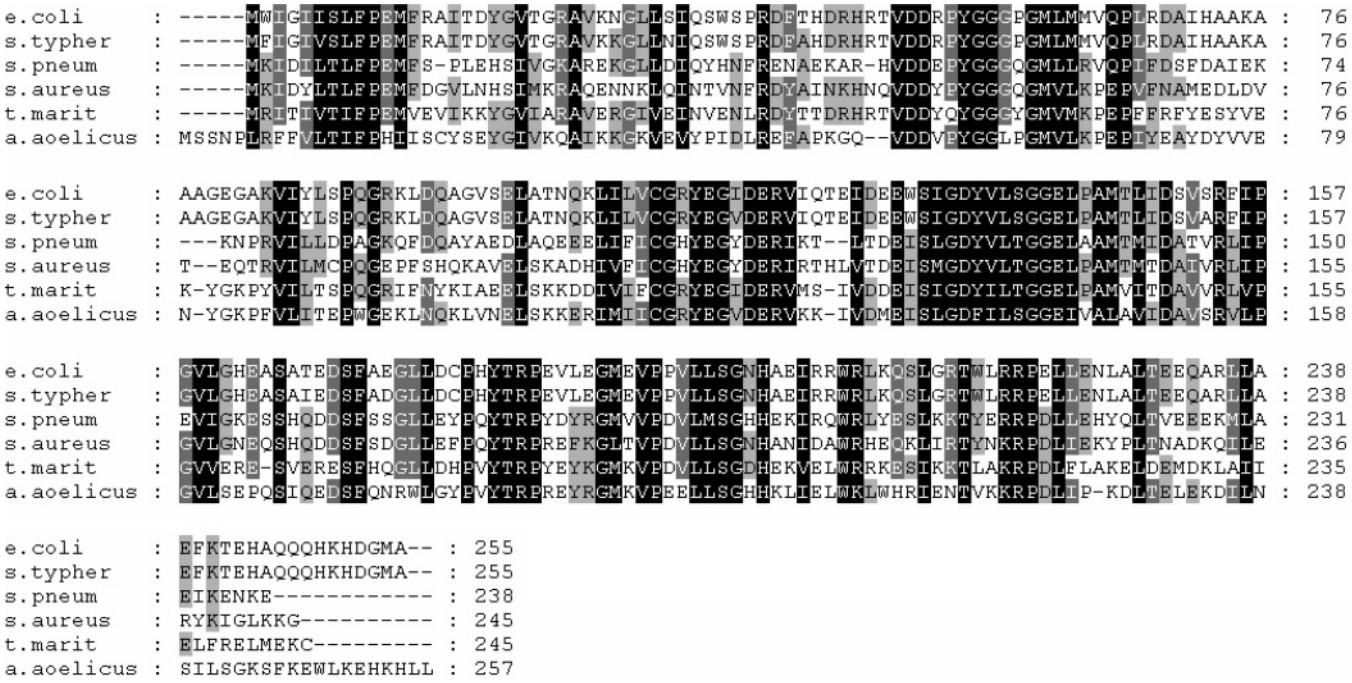


FIGURE 2: A ClustalW primary sequence alignment of a variety of differing bacterial *trmD* gene products.

Parallel reactions in the presence of the AdoMet analogue, sinefungin, were conducted. In all cases, the mixture was preincubated for 2 min, then lead acetate was added to a final concentration of 20 mM, and cleavage was carried out for 5 min. This high-lead concentration leads to RNA cleavage primarily in loop regions. The reaction was terminated by the addition of 33 mM EDTA and extracted in phenol/chloroform, and tRNA was precipitated with ethanol. In all experiments, equal quantities of labeled tRNA were cleaved. Enzyme and AdoMet were stable in the above cleavage mixture for at least 10 min. The products were run on an 8 M urea and 8 or 10% PAGE sequencing gel at approximately 900 V for 5 h.

*Fluorescence Resonance Energy Transfer*. All protein samples and substrate samples used in the following fluorescence experiments were in 50 mM Tris-HCl, pH 8.0, 100 mM KCl, 5 mM $MgCl_2$, 1 mM DTT, and 20% glycerol. Excitation and emission spectra at 25 °C were obtained using an AMINCO−Bowman spectrophotofluorometer at a fixed voltage determined by an initial auto-range function. In the same buffer, 25, 50, 75, and 100 $\mu$M concentrations of *S*-adenosyl-L-methionine absorbance spectra were obtained using a Beckman DU680B spectrophotometer to determine a wavelength of incident light which would not be absorbed during the FRET experiments; 285 nm was chosen. The various excitation and emission spectra and experimental outline are described in Figure 6.

*Modeling.* A visual representation of tRNA position 36 and 37 base conformational changes was accomplished by merging two Protein Databank files (PDB files) (Figure 8). Unmodified tRNA anticodon loop (protein data bank NMR structure: 1KKA (*17*)) was docked into a SYBYL (*41*) MOLCAD (*42*) surface rendition of dimeric TrmD (protein data bank crystal structure 1P9P (*4*)) created using three-dimensional modeling on a Silicon Graphics workstation. Rotation of bases 36 and 37 into the catalytic core was accomplished by rotating only one P−O3′ sigma bond of the "phosphodiester backbone" per base upon AdoMet binding site occupancy.

## RESULTS

*Primary Alignment.* ClustalW (*43*) primary amino acid sequence alignment showed over 60% sequence homology of TrmDs from a variety of differing organisms. It is important to note here that there is only one tryptophan per monomer at position 201 in *S. pneumonia* TrmD (Figure 2), which is shown later to be integral to FRET studies.

*tRNA Binding.* In our initial studies, we determined that very large amounts of *E. coli* enzyme (up to 200 $\mu$M) had to be added to achieve significant tRNA binding and protection. Such levels of *E. coli* enzyme did not permit us to carry out the fluorescence studies we wished to carry out given the high background contributed by the added protein. For example, if the $K_{app}$ for the *E. coli* enzyme was poor, then too much enzyme would have to be added to bind most of the tRNA present. Under these circumstances, quenching problems from added enzyme made such experiments impossible (data not shown). Therefore, it was important to determine which enzyme orthologs may be the best for ligand binding studies. As can be seen in Figure 3, there were great differences in $K_{d\,app}$ for the various orthologs. *E. coli* and *S. aureus* enzymes showed poor binding, giving a $K_{d\,app}$ of approximately 60 ± 6 $\mu$M with respect to TrmD concentration. *T. maritima* TrmD protein was bound much tighter with a $K_{d\,app}$ of 5 ± 1 $\mu$M with respect to TrmD concentration. *S. pneumoniae* TrmD showed the tightest binding of 500 ± 100 nM with respect to TrmD concentration, which is over 2 orders of magnitude tighter binding than seen using the *E. coli* or *S. aureus* enzyme. Therefore, the *Streptococcus* enzyme was utilized for FRET analyses. We should point out that when the three TrmD protein 3D structures are compared the degree of structural homology is remarkably conserved. This degree of homology implies a similar mechanism for all.

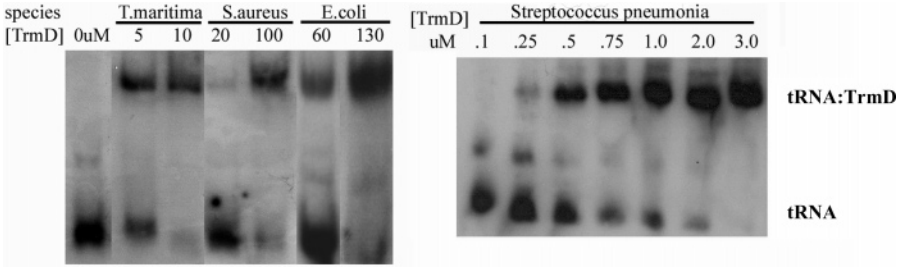


FIGURE 3: The 5% nondenaturing agarose gels, showing the ability of TrmD enzyme to bind and shift 5′-[$^{32}$P]-labeled $tRNA_1^{Leu}$ transcripts at various protein concentrations. Here, *S. pneumonia* TrmD shows greater than 30 times higher apparent affinity for tRNA than *E. coli* TrmD.

Sinefungin, a potent AdoMet analogue (Figure 1), competitively inhibits methylation by competing for occupancy at the AdoMet-binding site of methyltransferases. Obviously, tRNA footprinting experiments could not be done in the presence of enzyme and AdoMet, since the methylation reaction would be completed. Therefore, such experiments must be carried out in the presence of sinefungin.

First, it was determined what concentrations of sinefungin were required for inhibition of enzyme catalytic activity. Figure 4a shows that approximately 50 $\mu$M sinefungin was required to give 50% inhibition of enzyme activity under these conditions. Next, to test the effects of sinefungin on tRNA binding, gel-shift experiments were carried out (Figure 4b). A native gel-shift assay containing 5′-end labeled $tRNA_1^{Leu}$, increasing concentrations of *S. pneumoniae* TrmD, and up to 100 $\mu$M sinefungin was performed. Under these conditions, little or no effect on $tRNA_1^{Leu}$ transcript binding was observed (Figure 4b). This is consistent with previous kinetic studies, which suggested a random sequential mechanism where the binding of either substrate is not dependent on the presence of the other.

*Footprinting.* We previously have shown that *E. coli* TrmD protein binds and protects primarily the anticodon loop of $tRNA_1^{Leu}$ (*10*). In those experiments, it was noticed, surprisingly, that G36 and G37 residues were *not* protected against lead cleavage. These experiments were not done in the presence of excess AdoMet, since stable complexes could not be formed. We show here that occupancy of the AdoMet-binding site by sinefungin caused a substantial change in protection of residues of the anticodon stem against lead and enzyme cleavage including nucleotides 36 and 37.

Lead acetate cleaved after all nucleotides, with a preference for loops such as the anticodon, T-, and D-loops. Addition of 100 $\mu$M *E. coli* TrmD (over the experimentally determined $K_{d\ app}$) in the absence of sinefungin had little effect on G36/G37 cleavage patterns. This is in agreement with previously published footprinting which showed positions 36 and 37 are not protected by TrmD in the absence of AdoMet site occupancy (*10*). Figure 5c displays a complete gel of lead cleaved tRNA in the presence of enzyme and/or sinefungin. Here, some of the protection sites can be seen. However, when 3′-labeled tRNA is used and a closer view is given, it can be clearly seen that the addition of 50−200 $\mu$M sinefungin in the presence of the same TrmD concentration showed strong protection of the anticodon region of tRNA (residues 31−33, 35−37, 39, and 40) with a near total protection of the phosphodiester bonds of guanine residues 36 and 37 (Figure 5b). Even more dramatic was the protection seen when nuclease T2 was used to cleave labeled tRNA. Figure 5d shows that in the absence of sinefungin there is pronounced cleavage of the phosphodiester bonds associated with residues 33−36. In the presence of sinefungin, there is almost complete protection of these sites. These results show clearly that the tRNA backbone is perturbed in the presence of sinefungin, such that nuclease can no longer efficiently cleave tRNA at those sites. Note, also, that T2 nuclease cleaves at two sites (C34 and U33) where lead does not. This may reflect the complex structures of T2 or lead-tRNA/enzyme complexes required for maximal cleavage at any given residue.

*Fluorescence Analyses.* The above results strongly indicate that extensive protection of the phosphate backbone of the G37/G36 region of tRNA had occurred when the AdoMet site was fully occupied. This does not directly address the question of the environment of the G residues at positions 36 and 37. Therefore, another more direct approach (FRET) was employed to monitor movement of bases in these positions of the tRNA molecule. ClustalW (*43*) primary amino acid sequence alignment demonstrates over 60% sequence homology in a diverse number of organisms (Figure 1). Most importantly, it can be seen that there is only one tryptophan per monomer at position 201 of the *Streptococcal* TrmD protein. This is crucial for interpretation of the FRET analyses we shall describe.

Synthetic $tRNA_1^{Leu}$ substituted specifically at positions G36 and G37 with 2-aminopurine (36,37-2AP-$tRNA_1^{Leu}$) had significant spectral overlap between peptide emission and 2-aminopurine excitation. There was significant segregation of peptide excitation from AdoMet absorption and 2-aminopurine excitation allowing the use of this FRET experimental design. 2-Aminopurine emission gave a unique spectrum between 340 and 400 nm (Figure 6).

Mixtures containing 25−100 $\mu$M *S*-adenosylmethionine in 50 mM Tris-HCl, pH 8.0, 100 mM KCl, 5 mM MgCl2, 1 mM DTT, and 20% glycerol yielded an absorbance maximum at 260 nm but with less than 5% of the maximum absorbance at 280. At 285 nm, there was virtually no absorbance for up to 100 $\mu$M AdoMet (Figure 6). Therefore, 285 nm was chosen as the wavelength for incident light excitation. The excitation spectrum at 320 nm of *Streptococcal* TrmD protein showed a broad peak between 280 and 290 nm and emitted a typical protein emission (between 320 and 340 nm) upon 285 nm excitation, the difference of which is indicative of tryptophan emission (*44*). 2-Aminopurine-substituted tRNA excitation spectrum at 360 nm had a maximum of 320 nm; a typical 2-aminopurine emission spectrum between 350 and 400 nm, with a maximum at 360 nm, was displayed (*29*) when excited at 320 nm (Figure 6).

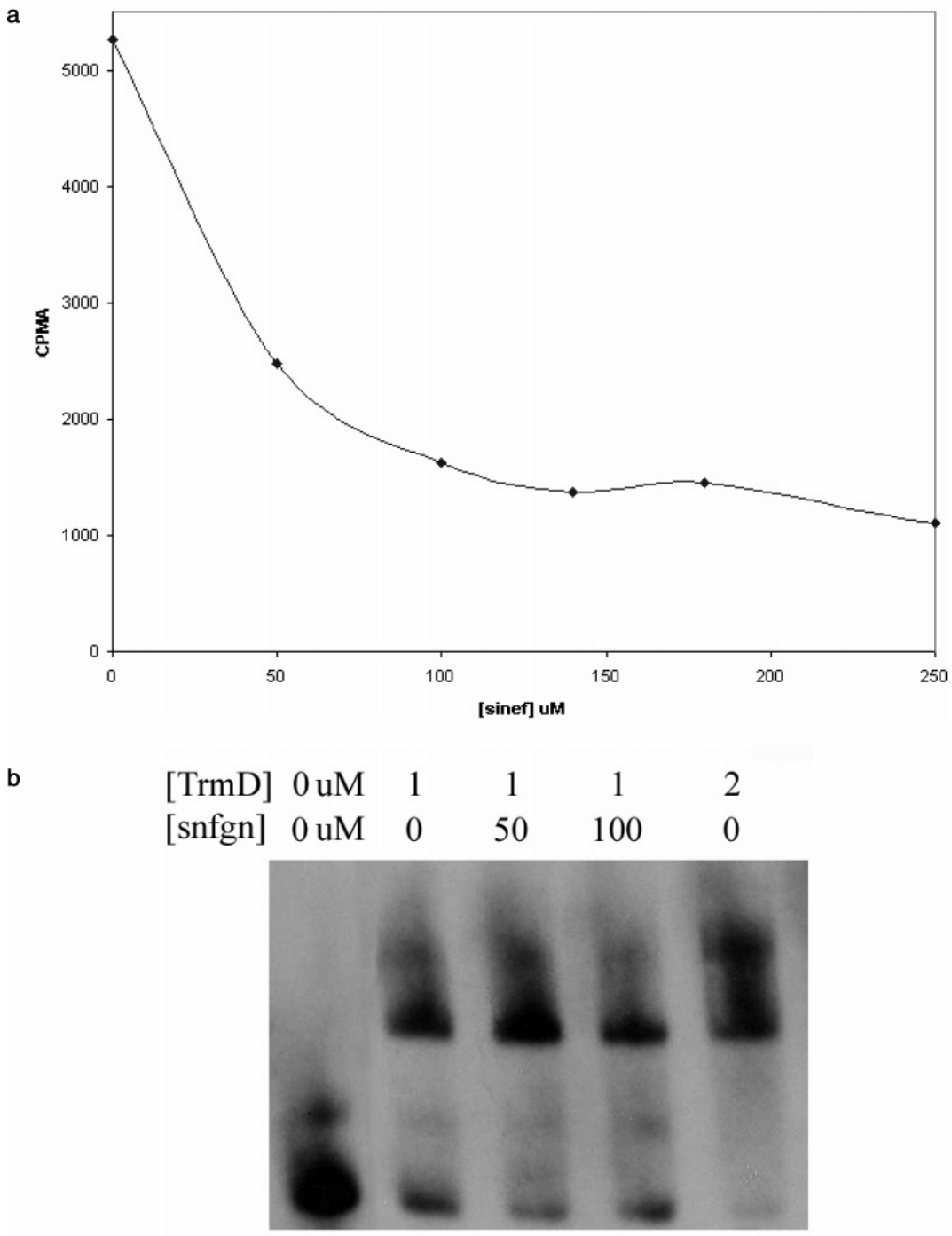


FIGURE 4: (a) An 8 min assay, containing 2 $\mu$M *S. pneumoniae* TrmD, 3.6 $\mu$M $tRNA_1^{Leu}$ transcript, and 15 $\mu$M *S*-adenosyl-L-methionine, was carried out with varying concentrations of sinefungin. (b**)** A gel-shift assay demonstrating 50 and 100 $\mu$M sinefungin concentrations have no effect on tRNA−TrmD interactions.

The obtained emission spectrum of *S. pneumoniae* TrmD upon excitation at 285 nm is exemplary of tryptophan fluorescence in the absence of AdoMet or tRNA (Figure 7a). Since there is only one tryptophan per monomer in the *Streptococcus* TrmD enzyme (position 201), changes in emission output and subsequent energy transfer can be attributed to a change of distance between W201 and the absorbing fluorophore, 2-aminopurine. The addition of 2AP-tRNA to the apoenzyme shifted the protein emission spectrum by decreasing the emission with a maximal decrease at 320 nm, and a range difference of which corresponds to 2AP-tRNA excitation, and by increasing the emission from 340 to 400 nm with a maximal change at 360 nm, corresponding to 2AP-tRNA emission. This indicates a transfer of energy from TrmD protein emission to 2AP-tRNA, followed by a fluorescence of 2-aminopurine. After an assay to show 36,37-2AP-tRNA was not methylated by TrmD (data not shown), increasing concentrations of *S*-adenosylmethionine were shown to decrease the emission between 340 and 400 nm, suggesting one or more of these two nucleotides at position 36 and 37 are moving further away from W201 upon the addition of AdoMet (Figure 7a). Fluorescence emission values at 360 nm for the *S. pneumoneae* energy transfer experiment decreased logarithmically as a function of AdoMet concentration with an apparent $K_m$ of 25 $\mu$M AdoMet (Figure 7b). This value correlated well

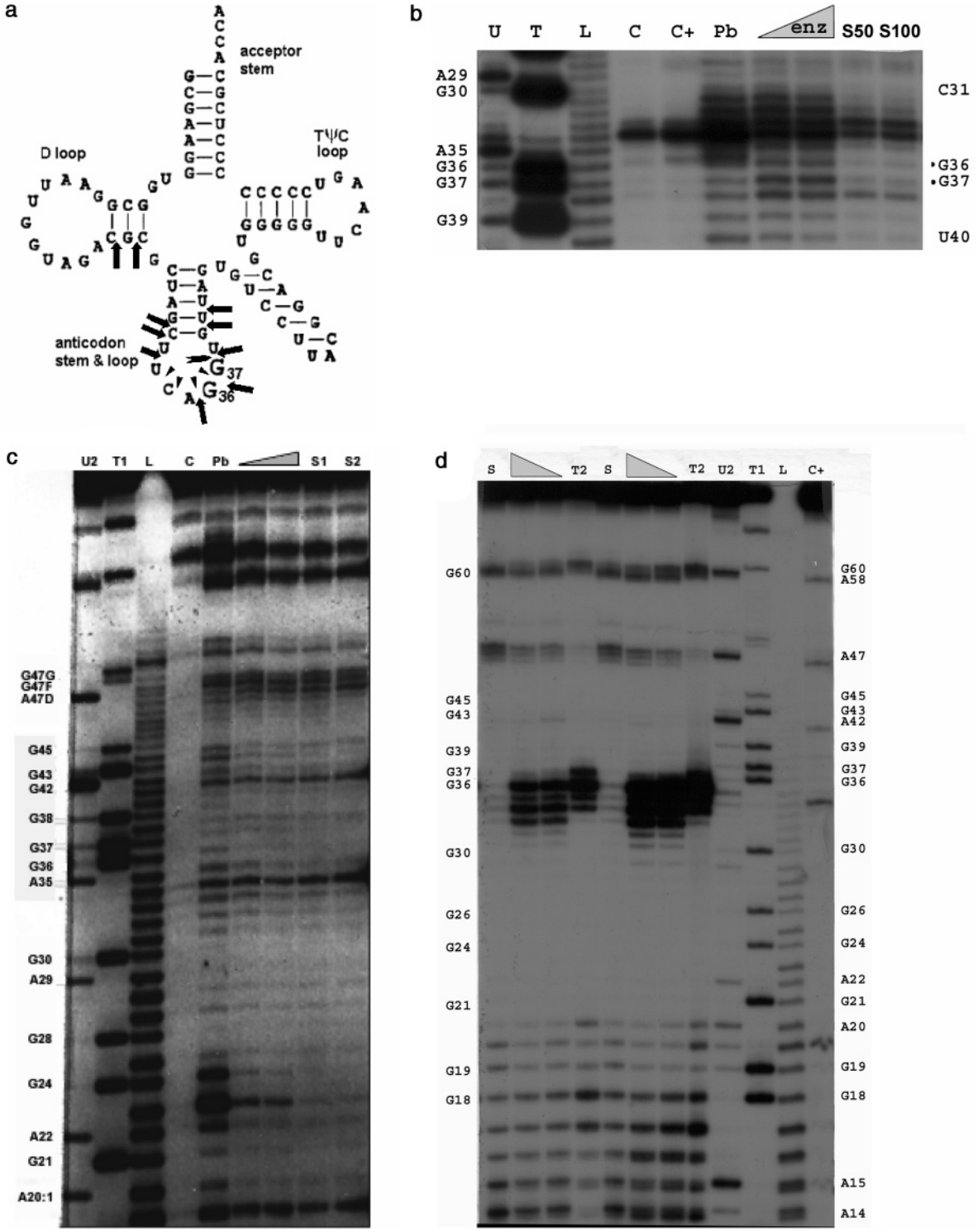


FIGURE 5: (a) tRNA cloverleaf displaying sites of lead and T2 enzyme cleavage. Solid arrows indicate sites for lead cleavage. Interior filled triangles indicate sites for T2 enzyme cleavage. The interior cleft arrow designates a site for T2 cleavage which is protected by the presence of TrmD enzyme alone. (b) TrmD protection against Pb cleavage. Experiment consisted of 3′-labeled transcript separated on 8% PAGE. From left to right: U, RNase U2 ladder; T, RNase T1 ladder; L, $H_2O$ ladder; C, control tRNA alone; C+, control tRNA in the presence of TrmD; Pb, tRNA alone treated with $Pb^{2+}$; full triangle, $Pb^{2+}$-treated complex of tRNA with 100 and 200 $\mu$g TrmD; S50 and S100, $Pb^{2+}$-treated complex of tRNA with 100 $\mu$M TrmD in the presence of sinefungin at 50 and 100 $\mu$M, respectively . (c) TrmD protection against Pb cleavage. From left to right: U2, U2 cleavage; T1, T1 cleavage; L, base hydrolysis ladder; C, 5′-labeled tRNA with no treatment; Pb, 5′-labeled tRNA cleaved with Pb; full triangle, tRNA plus 100 $\mu$g enzyme cleaved with Pb and tRNA plus 200 $\mu$g cleaved with lead; S1, tRNA plus 200 $\mu$g enzyme cleaved with Pb with 50 $\mu$M sinefungin; S2, tRNA plus 200 $\mu$g enzyme cleaved with Pb with 100 $\mu$M sinefungin. (d) 5′-Labeled transcript separated on 8% PAGE. From right to left: C+, control tRNA in the presence of TrmD; L, $H_2O$ ladder; T1, RNase T1 ladder; U2, RNase U2 ladder; T2, tRNA alone treated with 0.25 U $T_2$; triangle, 0.25 U $T_2$-treated complex of tRNA with increasing amounts of TrmD; S, 0.25 U $T_2$-treated complex of tRNA with 200 $\mu$M TrmD in the presence of 500 $\mu$M sinefungin; T2, tRNA alone treated with 0.5 U $T_2$; trangle, 5 U $T_2$-treated complex of tRNA with increasing amounts of TrmD; S, 0.5 U $T_2$-treated complex of tRNA with 200 $\mu$M TrmD in the presence of 500 $\mu$M sinefungin.

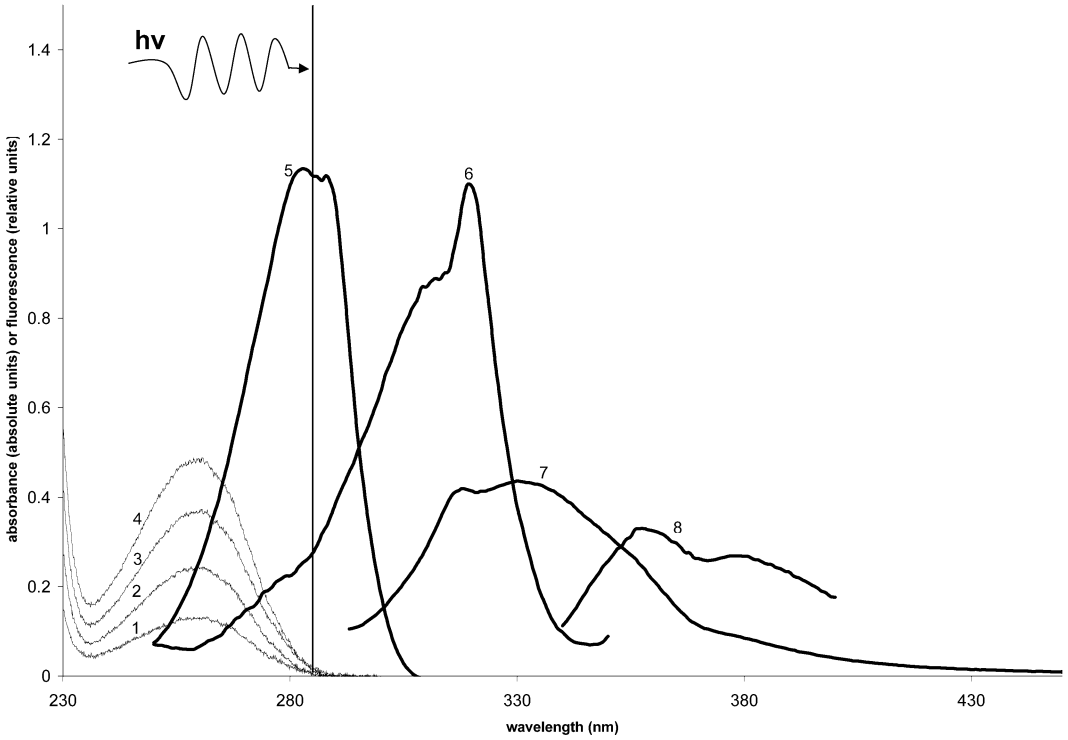


FIGURE 6: Resonance energy transfer experimental design. Curves 1, 2, 3, and 4 show absolute absorbance values for 25, 50, 75, and 100 $\mu$M *S*-adensosyl-L-methionine, respectively. Exciting light was provided at 285 nm, outside the absorbance values of AdoMet. Curve 5 shows the excitation spectrum at 320 nm of *Streptococcal* TrmD. Curve 6 is the excitation spectrum of 36,37-2-AP-substituted tRNA at 360 nm. Curve 7 is the emission spectrum of TrmD excited at 285 nm. Curve 8 is the emission spectrum of 36,37-2-AP-substituted tRNA excited at 320 nm.

with the kinetic AdoMet $K_m$ value for this enzyme (Figure 7b). When the emission values between 340 and 400 nm at three saturating concentrations of AdoMet are substracted, 2AP-tRNA−TrmD complexes yielded a spectrum that matched that of 2AP-tRNA alone upon excitation at 320 nm (Figure 7c). This indicates that this change in fluorescence reflects the emission of 2-aminopurine residues in the tRNA. The *E. coli* enzyme, which displayed a much lower affinity for tRNA via gel mobility shift analysis, did not alter the fluorescence emission of 2AP-tRNA upon the addition of up to 100 $\mu$M *S*-adenosylmethionine (data not shown). This was expected because the affinity of this ortholog for tRNA was poor. In addition, the *E. coli* enzyme has five tryptophan residues per monomer, which seriously complicates such analyses.

*Modeling.* The unmodified tRNA anticodon stem and loop NMR structure, (PDB NMR structure: 1KKA (*17*)) was docked into a MOLCAD (*42*) surface rendition of dimeric TrmD (protein data bank crystal structure 1P9P) (*4*), using a SiliconGraphics workstation and the program SYBYL (*41*) (Figure 8). Initial docking was successful with no van der Waals radius or steric violations. The anticodon stem/loop structure modeled is that of *E. coli* $tRNA^{Phe}$ which contains A36 and A37. Rotation of A36 and A37 into the catalytic core was accomplished by rotating only one P−O3′ sigma bond of the "phosphate backbone" per base; A36 was placed within 4 Å of AdoHcy's sulfur and A36 in a distinct pocket, which could account for position 36 specificity. This model matches a previously published model which used crystallization, site directed mutagenesis, and catalytic studies and indicated likely positions of 36 and 37 (*4*). *S. pneumoniae*'s single tryptophan, W201, is positioned near tRNA positions 36 and 37 prior to rotation after AdoMet binding, where the two residues were moved deeper into the catalytic pocket and further away from W201. This tRNA anticodon conformational change model upon occupancy of the AdoMet-binding site matches the footprinting and FRT experiments previously described.

## DISCUSSION

We have shown here that substantial changes in tRNA−protein complex structure accompany the binding of AdoMet as revealed by probing experiments and FRET analysis. The probing experiments show clearly that substantial portions of the anticodon stem and loop phosphodiester backbone become protected but do not directly address the movement of bases associated with these protected regions. Therefore, FRET analysis was carried out.

During the course of these studies we found that the *E. coli* enzyme displayed a relatively poor affinity for tRNA as compared to several TrmD orthologs reported on here. This precluded the use of the *E. coli* enzyme for FRET studies since enzyme concentrations required to saturate tRNA precluded this approach. However, the *E. coli* TrmD protein was suitable for lead probing studies since very high levels of enzyme could be added without interfering with the measurements being made. The *Streptococcal* enzyme was chosen for FRET analysis because tRNA affinities were excellent and also because this ortholog has only one tryptophan per monomer. Therefore, any FRET seen could be more directly attributed to relative changes in distance between the sole tryptophan and 2-aminopurine in the bound tRNA.

Bacterial TrmD, tRNA methyltransferase, structural features are highly conserved at the level of primary amino acid

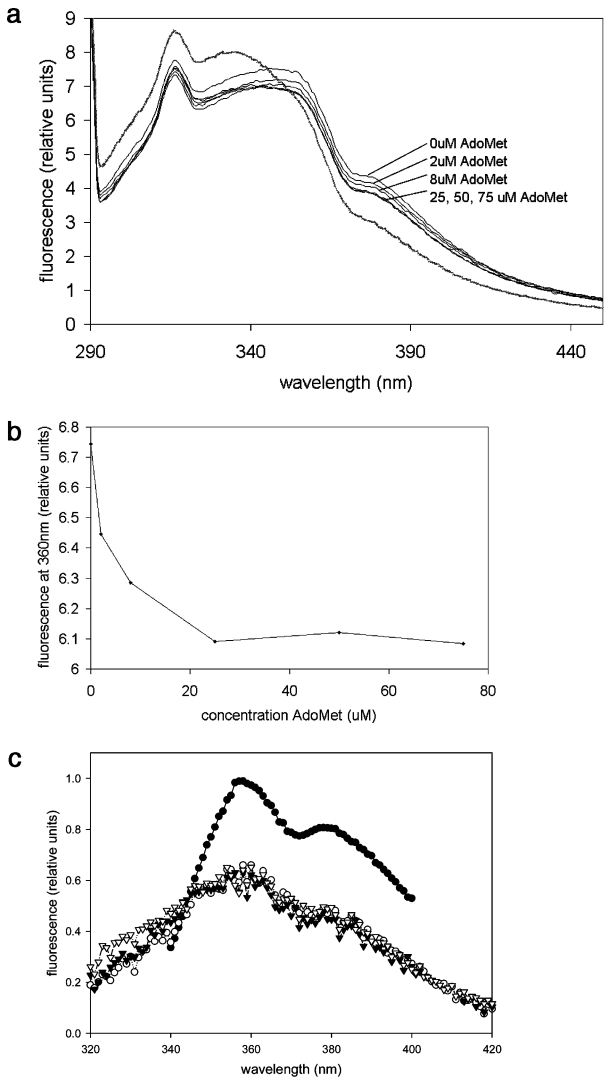


FIGURE 7: (a) The effect of increasing concentrations of AdoMet on fluorescence emission spectra of *Streptococcal* TrmD protein complexed with 2AP tRNA; the emission profile of enzyme alone is depicted as the thick gray line. (b) Fluorescence emission values of enzyme−2AP-tRNA complexes at 360 nm as a function of AdoMet concentration. Maximal quenching is observed at 25 $\mu$M AdoMet. (c) The emission spectrum of 2AP-substituted tRNA alone (solid circles) at 320 nm is compared to the spectrum obtained in the presence of enzyme and three concentrations (25, 50, and 75 $\mu$M) of saturating AdoMet (open circles, open trangles, and closed triangles, respectively). Here, values obtained in the presence of saturating concentrations of AdoMet have been subtracted from values obtained in the absence of added AdoMet.

sequence, and even more so when three-dimensional structures are compared. Three mesophilic, eubacterial structures have been determined, *Haemophilus influenzae* (*45*), *E. coli* (*4*), and *S. aureus* (unpublished data, this laboratory), and all three have near identical tertiary structure. Therefore, the differences in apparent binding of the various organisms' *trmD* gene products on a nondenaturing acrylamide gel must be subtle and involve individual residues rather than global differences in tertiary structure. The area of greatest primary sequence divergence is the C-terminal end of the protein, which has been postulated to contact the tRNA core region (*4*). Therefore, the heterogeneity in these regions could account for the observed differences in $K_{app}$ for tRNA via gel mobility shift assays.

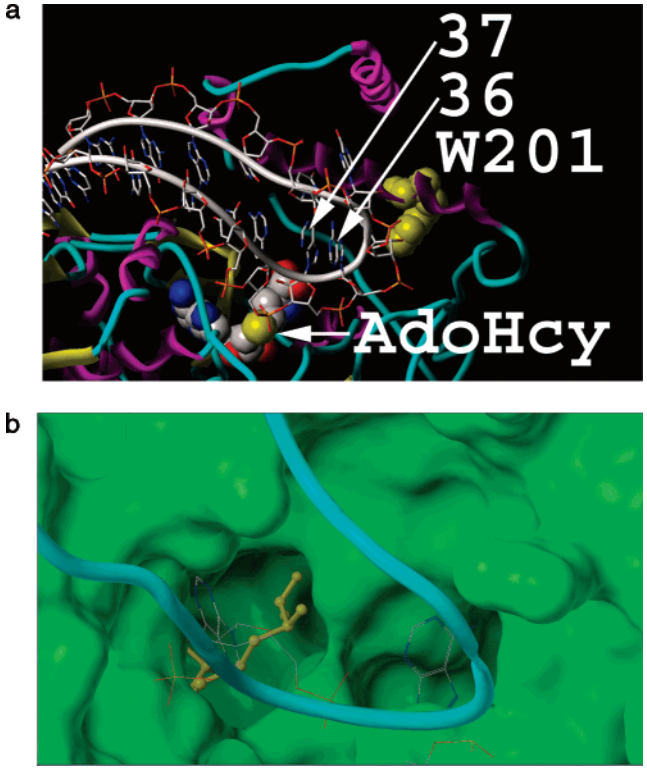


FIGURE 8: Visual representation of aminopurine bases 36 and 37 near the TrmD catalytic center. (a) A putative structure of the ALS before base rotation with the surface removed. The ribbon diagram of the TrmD backbone is shown in cyan and magenta; the single *Streptococcus* TrmD tryptophan residue, W201, is shown in yellow as a space filling model. Rotation of AP36pAP37 after occupancy of the AdoMet-binding site places these bases further from the fluorescing trytophan. Here, an unmodified tRNA anticodon loop is docked into a rendition of TrmD (protein data bank crystal structure 1P9P). (b) A view of the active site after rotation of 2AP37 to within 4 Å of AdoHcy. Here also 2AP36 is modeled into a distinct adjacent pocket, which could account for position 36 specificity. Rotation of AP36 and AP37 into the catalytic core was accomplished by rotating only one P−O3′ $\sigma$-bond of the "phosphate backbone" per base.

The observed AdoMet-dependent lead cleavage protection of the anticodon stem/loop including G36pG37 could require either enzyme isomerization involving peptide localization over the anticodon region or a local conformational change in the transfer RNA itself, bringing the anticodon nucleotides deep into the protein. In accordance with previous observations in the literature, and our FRET studies reported here, it becomes apparent that the latter is more likely. First, the *H. influenzae* TrmD enzyme has been crystallized in the presence and absence of *S*-adenosylmethionine or *S*-adenosylhomocysteine, and no major conformational change between the three structures was observed (*45*). Second, the various reported crystal structures of TrmD proteins show low *B*-values around the AdoMet-binding active site, suggesting this area is rather static with or without AdoMet. Finally, the anticodon region of several tRNA molecules has been shown directly by NMR to be highly mobile in the presence of magnesium (*46*, *22*, *25*), which is a necessary component for in vitro catalysis by TrmD (*2*, *6*).

The FRET studies presented here further support the notion of transfer RNA undertaking the majority of the dynamics necessary to properly position G37 and/or G36 into the catalytic cleft. Previous studies have shown that position 36

must be a purine in order for catalysis to proceed. Initially, addition of 36,37-2AP-tRNA causes a shift in emission from peptidyl tryptophan residue to 2-aminopurine, resulting in an increase in 2-aminopurine fluorescence due to spectral overlap of protein emission and 36,37-2AP-tRNA excitation. Upon addition of AdoMet to the protein−36,37-2AP-tRNA complex, the efficiency of fluorescence energy transfer from tryptophan 201 to guanine 36 and 37 is decreased in the *Streptococcal* system (Figure 7a). Since there are two aminopurine residues in tRNA in these experiments, it is not possible to determine an absolute Förster distance, $R_o$. The Förster equation $E = (R_o)^6/(R^6 + (R_o)^6)$ (*47*) dictates that energy transfer, *E*, is a function only of the distance between an emitting and absorbing fluorophore, since $R_o$ for any given system is a constant (*48*). Therefore, a decrease of fluorescence transfer between W201 and 36,37-2AP-tRNA correlates with an increase in distance between the nucleotides 36 and 37 and the only tryptophan (W201) in *S. pneumoniae* TrmD. It should be pointed out that the *E. coli* TrmD protein, which binds tRNA much less avidly than the *Streptococcal* enzyme and has four tryptophans per monomer, did not show a decrease in fluorescence energy transfer with the addition of up to 100 $\mu$M AdoMet (data not shown). This was not unexpected since the tRNA binding $K_d$ for the *E. coli* enzyme is over 2 orders of magnitude higher than that for the *Streptococcal* enzyme. Therefore, too much enzyme would have to be added to realize a measurable change in FRET in view of the significant overlap between protein and 2AP emissions at 360 nm (Figure 6).

Three-dimensional modeling displays a visual representation of the increase of distance between W201 and 36,37-2AP-tRNA. W201 lies in the middle of an inflexible α-helix present in the C-terminal domain of each subunit (Figure 8). Finally, this conserved tryptophan does not change position in the presence or absence of bound AdoMet (*45*).

The unmodified anticodon stem/loop 1KKA NMR structure fits well into the Trm catalytic cleft, and upon rotation of phosphate bonds flanking position 36 and 37, A37 becomes positioned within 4 Å of AdoMet, such that N1 of this adenine residue is proximal to the methyl group of AdoMet. In addition, A36 may move into a distinct pocket which could account for position 36 specificity for purines. These locations of nucleotides 36 and 37 agree with the previously published 3D model of guanine−phosphoguanosine which was determined via in silico modeling into the crystal structure and site directed mutagenesis of the regions (*4*). This current model visually explains the decrease in energy transfer from tryptophan 201 to 2-aminopurine.

Two recent publications dealing with the interaction of tRNA and cognate modification enzymes have demonstrated that substantial changes in tRNA structure accompany catalysis (26, 27). In these cases, cocrystal structures establish the exact nature of these changes. Hoang et al. (26) have shown that the TruB enzyme recognizes the T-loop structure and, upon binding, "flips" the FU55 residue out of the structure in order to carry out the appropriate isomerization. It appears that fluorouridine, which can serve as a substrate, may not permit the release of tRNA and permits the formation of a stabile intermediate. This was the first documentation that RNA modification enzymes could carry out flipping. It was noted that the base to be modified was moved deep into the catalytic cleft of the enzyme.

Even more extensive changes in tRNA structure accompany complex formation with the ArcTGT enzyme. Here, the G15 residue is removed from deep within the tRNA structure for molecular replacement with queosine (27). The complete D-loop is moved outward, now rendering the G15 residue available for subsequent catalysis. In both these cases, it is clear that the enzyme alone is capable of disrupting tRNA structure. It will be interesting to determine what further structural changes will occur in the ArcTGT enzyme in the presence of queosine. This will, of course, require the availability of some suitable analogue which might trigger further structural changes required for archaeosine synthesis and tRNA release.

Here, we have shown for the first time that an analogue of a substrate for tRNA modification can trigger tRNA structural changes which are quite stabile, since probe experiments clearly reveal changes in the environment of appropriate sites in tRNA. It will be important for future studies to obtain a crystal structure of TrmD complexed with tRNA. We anticipate that movement of the G37 base into the catalytic center will indeed require occupancy of the AdoMet binding site. Ultimately, it is hoped that such studies will illuminate mechanisms whereby proteins can dramatically alter the structure of DNA or RNA.

## REFERENCES


1. Bystrom, A. S., and Bjork, G. R. (1982) Chromosomal location and cloning of the gene (*trmd*) responsible for the synthesis of tRNA (m1g) methyltransferase in *Escherichia coli* k-12, *Mol. Gen. Genet. 188*, 440−6.
2. Holmes, W. M., Andraos-Selim, C., Roberts, I., and Wahab, S. Z. (1992) Structural requirements for tRNA methylation. Action of *Escherichia coli* tRNA(guanosine-1)methyltransferase on tRNA-(1leu) structural variants, *J. Biol. Chem. 267*, 13440−5.
3. Brule, H., Elliott, M., Redlak, M., Zehner, Z. E., and Holmes, W. M. (2004) Isolation and characterization of the human tRNA-(n1g37) methyltransferase (trm5) and comparison to the *Escherichia coli* TrmD protein, *Biochemistry 43*, 9243−55.
4. Elkins, P. A., Watts, J. M., Zalacain, M., van Thiel, A., Vitazka, P. R., Redlak, M., Andraos-Selim, C., Rastinejad, F., and Holmes, W. M. (2003) Insights into catalysis by a knotted TrmD tRNA methyltransferase, *J. Mol. Biol. 333*, 931−49.
5. Bjork, G. R., Wikstrom, P. M., and Bystrom, A. S. (1989) Prevention of translational frameshifting by the modified nucleoside 1-methylguanosine, *Science 244*, 986−9.
6. O'Dwyer, K., Watts, J. M., Biswas, S., Ambrad, J., Barber, M., Brule, H., Petit, C., Holmes, D. J., Zalacain, M., and Holmes, W. M. (2004) Characterization of *Streptococcus pneumoniae trmd*, a tRNA methyltransferase essential for growth, *J. Bacteriol. 186*, 2346−54.
7. Bjork, G. R., Jacobsson, K., Nilsson, K., Johansson, M. J., Bystrom, A. S., and Persson, O. P. (2001) A primordial tRNA modification required for the evolution of life? *EMBO J. 20*, 231−9.
8. Persson, B. C., Bylund, G. O., Berg, D. E., and Wikstrom, P. M. (1995) Functional analysis of the *ffh-trmd* region of the *Escherichia coli* chromosome by using reverse genetics, *J. Bacteriol. 177*, 5554−60.
9. Kobayashi, K., Ehrlich, S. D., Albertini, A., Amati, G., Andersen, K. K., Arnaud, M., Asai, K., Ashikaga, S., Aymerich, S., Bessieres, P., Boland, F., Brignell, S. C., Bron, S., Bunai, K., Chapuis, J., Christiansen, L. C., Danchin, A., Debarbouille, M., Dervyn, E., Deuerling, E., Devine, K., Devine, S. K., Dreesen, O., Errington, J., Fillinger, S., Foster, S. J., Fujita, Y., Galizzi, A., Gardan, R., Eschevins, C., Fukushima, T., Haga, K., Harwood, C. R., Hecker, M., Hosoya, D., Hullo, M. F., Kakeshita, H., Karamata, D., Kasahara, Y., Kawamura, F., Koga, K., Koski, P., Kuwana, R., Imamura, D., Ishimaru, M., Ishikawa, S., Ishio, I., Le Coq, D., Masson, A., Mauel, C., Meima, R., Mellado, R. P., Moir, A., Moriya, S., Nagakawa, E., Nanamiya, H., Nakai, S., Nygaard, P., Ogura, M., Ohanan, T., O'Reilly, M., O'Rourke, M., Pragai, Z.,

Pooley, H. M., Rapoport, G., Rawlins, J. P., Rivas, L. A., Rivolta, C., Sadaie, A., Sadaie, Y., Sarvas, M., Sato, T., Saxild, H. H., Scanlan, E., Schumann, W., Seegers, J. F., Sekiguchi, J., Sekowska, A., Seror, S. J., Simon, M., Stragier, P., Studer, R., Takamatsu, H., Tanaka, T., Takeuchi, M., Thomaides, H. B., Vagner, V., van Dijl, J. M., Watabe, K., Wipat, A., Yamamoto, H., Yamamoto, M., Yamamoto, Y., Yamane, K., Yata, K., Yoshida, K., Yoshikawa, H., Zuber, U., and Ogasawara, N. (2003) Essential *Bacillus subtilis* genes, *Proc. Natl. Acad. Sci. U.S.A. 100*, 4678−83.

10. Gabryszuk, J., and Holmes, W. M. (1997) TRNA recognition for modification: solution probing of tRNA complexed with *Escherichia coli* tRNA (guanosine-1) methyltransferase, *Rna 3*, 1327−36.
11. Robertus, J. D., Ladner, J. E., Finch, J. T., Rhodes, D., Brown, R. S., Clark, B. F., and Klug, A. (1974) Structure of yeast phenylalanine tRNA at 3 Å resolution, *Nature 250*, 546−51.
12. Jack, A., Ladner, J. E., and Klug, A. (1976) Crystallographic refinement of yeast phenylalanine transfer RNA at 2−5 Å resolution, *J. Mol. Biol. 108*, 619−49.
13. Hingerty, B., Brown, R. S., and Jack, A. (1978) Further refinement of the structure of yeast tRNAphe, *J. Mol. Biol. 124*, 523−34.
14. Klimasauskas, S., Kumar, S., Roberts, R. J., and Cheng, X. (1994) Hhai methyltransferase flips its target base out of the DNA helix, *Cell 76*, 357−69.
15. Shi, H., and Moore, P. B. (2000) The crystal structure of yeast phenylalanine tRNA at 1.93 Å resolution: a classic structure revisited, *RNA 6*, 1091−105.
16. Stuart, J. W., Gdaniec, Z., Guenther, R., Marszalek, M., Sochacka, E., Malkiewicz, A., and Agris, P. F. (2000) Functional anticodon architecture of human tRNAlys3 includes disruption of intraloop hydrogen bonding by the naturally occurring amino acid modification, t6a, *Biochemistry 39*, 13396−404.
17. Cabello-Villegas, J., Winkler, M. E., and Nikonowicz, E. P. (2002) Solution conformations of unmodified and a(37)n(6)-dimethylallyl modified anticodon stem-loops of *Escherichia coli* tRNA(phe), *J. Mol. Biol. 319*, 1015−34.
18. Yarian, C. S., Basti, M. M., Cain, R. J., Ansari, G., Guenther, R. H., Sochacka, E., Czerwinska, G., Malkiewicz, A., and Agris, P. F. (1999) Structural and functional roles of the n1- and n3-protons of psi at tRNA's position 39, *Nucleic Acids Res. 27*, 3543−9.
19. Adamiak, D. A., Rypniewski, W. R., Milecki, J., and Adamiak, R. W. (2001) The 1.19 Å X-ray structure of 2′−o-me(cgcgcg)(2) duplex shows dehydrated RNA with 2-methyl-2,4-pentanediol in the minor groove, *Nucleic Acids Res. 29*, 4144−53.
20. Yap, L. P., and Musier-Forsyth, K. (1995) Transfer RNA aminoacylation: identification of a critical ribose 2′-hydroxyl-base interaction, *RNA 1*, 418−24.
21. Micura, R., Pils, W., Hobartner, C., Grubmayr, K., Ebert, M. O., and Jaun, B. (2001) Methylation of the nucleobases in RNA oligonucleotides mediates duplex-hairpin conversion, *Nucleic Acids Res. 29*, 3997−4005.
22. Stuart, J. W., Koshlap, K. M., Guenther, R., and Agris, P. F. (2003) Naturally-occurring modification restricts the anticodon domain conformational space of tRNA(phe), *J. Mol. Biol. 334*, 901−18.
23. Bjork, G. R., Ericson, J. U., Gustafsson, C. E., Hagervall, T. G., Jonsson, Y. H., and Wikstrom, P. M. (1987) Transfer RNA modification, *Annu. Rev. Biochem. 56*, 263−87.
24. Nissen, P., Kjeldgaard, M., Thirup, S., Polekhina, G., Reshetnikova, L., Clark, B. F., and Nyborg, J. (1995) Crystal structure of the ternary complex of phe-tRNAphe, ef-tu, and a gtp analog. *Science 270*, 1464−72.
25. Cabello-Villegas, J., Tworowska, I., and Nikonowicz, E. P. (2004) Metal ion stabilization of the u-turn of the a37 n6-dimethylallyl-modified anticodon stem-loop of *Escherichia coli* tRNAphe, *Biochemistry 43*, 55−66.
26. Hoang, C., and Ferre-D'Amare, A. R. (2001) Cocrystal structure of a tRNA psi55 pseudouridine synthase: nucleotide flipping by an RNA-modifying enzym, *Cell 107*, 929−39.
27. Ishitani, R., Nureki, O., Nameki, N., Okada, N., Nishimura, S., and Yokoyama, S. (2003) Alternative tertiary structure of tRNA for recognition by a posttranscriptional modification enzyme, *Cell 113*, 383−94.
28. Ward, D. C., Reich, E., and Stryer, L. (1969) Fluorescence studies of nucleotides and polynucleotides. I. Formycin, 2-aminopurine riboside, 2,6-diaminopurine riboside, and their derivatives, *J. Biol. Chem. 244*, 1228−37.
29. Holz, B., Klimasauskas, S., Serva, S., and Weinhold, E. (1998) 2-Aminopurine as a fluorescent probe for DNA base flipping by methyltransferases, *Nucleic Acids Res. 26*, 1076−83.
30. Cheng, X., and Blumenthal, R. M., Eds. (1999) *S-Adenosylmethionine-Dependent Methyltrasferases: Structures and Functions*, World Scientific Pub Co., River, Edge, NJ.
31. Cheng, X., and Roberts, R. J. (2001) Adomet-dependent methylation, DNA methyltransferases and base flipping, *Nucleic Acids Res. 29*, 3784−95.
32. Guest, C. R., Hochstrasser, R. A., Sowers, L. C., and Millar, D. P. (1991) Dynamics of mismatched base pairs in DNA, *Biochemistry 30*, 3271−9.
33. Xu, D., Evans, K. O., and Nordlund, T. M. (1994) Melting and premelting transitions of an oligomer measured by DNA base fluorescence and absorption, *Biochemistry 33*, 9592−9.
34. Christine, K. S., MacFarlane, A. W. T., Yang, K., and Stanley, R. J. (2002) Cyclobutylpyrimidine dimer base flipping by DNA photolyase, *J. Biol. Chem. 277*, 38339−44.
35. Selvin, P. R. (2000) The renaissance of fluorescence resonance energy transfer, *Nat. Struct. Biol. 7*, 730−4.
36. Redlak, M., Andraos-Selim, C., Giege, R., Florentz, C., and Holmes, W. M. (1997) Interaction of tRNA with tRNA (guanosine-1)methyltransferase: binding specificity determinants involve the dinucleotide g36pg37 and tertiary structure, *Biochemistry 36*, 8699−709.
37. Altschul, S. F., Gish, W., Miller, W., Myers, E. W., and Lipman, D. J. (1990) Basic local alignment search too, *J. Mol. Biol. 215*, 403−10.
38. Clarke, P. (1999) Labeling and purification of RNA synthesized by in vitro transcription, in *Rna-Protein Interaction Protocols* (Haynes, S., Ed.) pp 1−10, Humana Press, Inc., Totowa, NJ.
39. Silberklang, M., Prochiantz, A., Haenni, A. L., and Rajbhandary, U. L. (1977) Studies on the sequence of the 3′-terminal region of turnip-yellow-mosaic-virus RNA, *Eur. J. Biochem. 72*, 465−78.
40. Setzer, D. R. (1999) Measuring equilibrium and kinetic constants using gel retardation assays, *Methods Mol. Biol. 118*, 115−28.
41. *Sybyl*, version 6.8, Tripos Inc., St. Louis, MO, .
42. Brickmann, J. G. T., Heiden, W., and Waldherr-Techner, M. (1992) Examining and manipulating molecular surfaces: generation and manipulation of solid models with the MOLCAD molecular graphics system, *J. Mol. Graph. 10*, 35.
43. Thompson, J. D., Higgins, D. G., and Gibson, T. J. (1994) Clustal w: improving the sensitivity of progressive multiple sequence alignment through sequence weighting, position-specific gap penalties and weight matrix choice, *Nucleic Acids Res. 22*, 4673−80.
44. Valeur, B. (2002) *Molecular Fluorescence: Principles and Applications*, Wiley-VCH, Weinheim and New York.
45. Ahn, H. J., Kim, H. W., Yoon, H. J., Lee, B. I., Suh, S. W., and Yang, J. K. (2003) Crystal structure of tRNA(m1g37)methyltransferase: insights into tRNA recognition, *EMBO J. 22*, 2593−603.
46. Schweisguth, D. C., and Moore, P. B. (1997) On the conformation of the anticodon loops of initiator and elongator methionine tRNAs, *J. Mol. Biol. 267*, 505−19.
47. dos Remedios, C. G., and Moens, P. D. (1995) Fluorescence resonance energy transfer spectroscopy is a reliable "ruler" for measuring structural changes in proteins. Dispelling the problem of the unknown orientation factor, *J. Struct. Biol. 115*, 175−85.
48. Lakowicz, J. R. (1999) *Principles of Fluorescence Spectroscopy*, 2nd ed., Kluwer Academic/Plenum, New York.

BI0481038